

J/ Elliptic Flow in Pb-Pb Collisions at $\sqrt{s_{NN}}=5.02$ TeV

著者別名	ブッシュ オリバー, 中條 達也, 三明 康郎, 坂井 真吾
journal or publication title	Physical review letters
volume	119
number	24
page range	242301
year	2017-12
権利	(C) 2017 CERN, for the ALICE Collaboration Published by the American Physical Society under the terms of the Creative Commons Attribution 4.0 International license. Further distribution of this work must maintain attribution to the author(s) and the published article's title, journal citation, and DOI.
URL	http://hdl.handle.net/2241/00150721

doi: 10.1103/PhysRevLett.119.242301

J/ψ Elliptic Flow in Pb-Pb Collisions at $\sqrt{s_{NN}} = 5.02$ TeVS. Acharya *et al.*^{*}
(ALICE Collaboration)

(Received 27 September 2017; revised manuscript received 7 November 2017; published 15 December 2017)

We report a precise measurement of the J/ψ elliptic flow in Pb-Pb collisions at $\sqrt{s_{NN}} = 5.02$ TeV with the ALICE detector at the LHC. The J/ψ mesons are reconstructed at midrapidity ($|y| < 0.9$) in the dielectron decay channel and at forward rapidity ($2.5 < y < 4.0$) in the dimuon channel, both down to zero transverse momentum. At forward rapidity, the elliptic flow v_2 of the J/ψ is studied as a function of the transverse momentum and centrality. A positive v_2 is observed in the transverse momentum range $2 < p_T < 8$ GeV/ c in the three centrality classes studied and confirms with higher statistics our earlier results at $\sqrt{s_{NN}} = 2.76$ TeV in semicentral collisions. At midrapidity, the J/ψ v_2 is investigated as a function of the transverse momentum in semicentral collisions and found to be in agreement with the measurements at forward rapidity. These results are compared to transport model calculations. The comparison supports the idea that at low p_T the elliptic flow of the J/ψ originates from the thermalization of charm quarks in the deconfined medium but suggests that additional mechanisms might be missing in the models.

DOI: 10.1103/PhysRevLett.119.242301

Extreme conditions of temperature and pressure created in ultrarelativistic heavy-ion collisions enable the exploration of the phase diagram region where quantum chromodynamics (QCD) predicts the existence of a deconfined state, the quark-gluon plasma (QGP) [1,2]. Heavy quarks are produced through hard-scattering processes prior to the formation of the QGP and experience the evolution through interactions in the medium. Therefore, the measurement of bound states of heavy quarks, such as the J/ψ , is expected to provide sensitive probes of the strongly interacting medium [3]. Theoretical calculations based on lattice QCD predict a J/ψ suppression to be induced by the screening of the color force in a deconfined medium which becomes stronger as the temperature increases [4,5]. In a complementary way to this static approach, J/ψ suppression can be also interpreted as the result of dynamical interactions with the surrounding partons [6–8]. Within these scenarios, the J/ψ suppression, experimentally quantified via the nuclear modification factor R_{AA} (the ratio between the yields in Pb-Pb to pp collisions normalized by the number of nucleon-nucleon collisions), is expected to become stronger (smaller R_{AA}) with higher initial temperatures of the QGP and, hence, with higher collision energies. However, the R_{AA} of inclusive J/ψ with transverse momentum $p_T < 8$ GeV/ c observed by the ALICE Collaboration in Pb-Pb collisions at

$\sqrt{s_{NN}} = 2.76$ TeV [9] and $\sqrt{s_{NN}} = 5.02$ TeV [10] is larger than what has been measured at lower energies at the Relativistic Heavy Ion Collider (RHIC) [11–14] and exhibits almost no centrality dependence. [Inclusive J/ψ include prompt J/ψ (direct and decays from higher mass charmonium states) and nonprompt J/ψ (feed down from b -hadron decays). In this Letter, all J/ψ measurements refer to inclusive J/ψ production unless otherwise stated.] Furthermore, in central collisions the measured R_{AA} values decrease from low to high p_T [15,16]. The J/ψ R_{AA} enhancement from RHIC to LHC energies can be explained by theoretical models [6–8,17–19] which include a dominant contribution from J/ψ (re)generation through the (re) combination of thermalized charm quarks in the medium, during or at the phase boundary of the deconfined phase. [The terms (re)generation and (re)combination denote the two possible mechanisms of J/ψ generation by the combination of charm quarks at the QGP phase boundary and the continuous dissociation and recombination of charm quarks during the QGP evolution.]

Additional observables are required to better constrain theoretical models and study the interplay between suppression and regeneration mechanisms [20]. The azimuthal anisotropy of the final-state particle momentum distribution is sensitive to the geometry and the dynamics of the early stages of the collisions. The spatial anisotropy in the initial matter distribution due to the nuclear overlap region in noncentral collisions is transferred to the final momentum distribution via multiple collisions in a strongly coupled system [21]. The beam axis and the impact parameter vector of the colliding nuclei define the reaction plane. The second coefficient (v_2) of the Fourier expansion of the final-state particle azimuthal distribution with respect to the reaction plane is called elliptic flow.

^{*}Full author list given at the end of the article.

Published by the American Physical Society under the terms of the [Creative Commons Attribution 4.0 International license](https://creativecommons.org/licenses/by/4.0/). Further distribution of this work must maintain attribution to the author(s) and the published article's title, journal citation, and DOI.

Within the transport model scenario [7,19], (re)generated J/ψ inherit the flow of the (re)combined charm quarks. If charm quarks do thermalize in the QGP, then (re)generated J/ψ can exhibit a large elliptic flow. In contrast, only a small azimuthal anisotropy, due to the shorter in-plane versus out-of-plane path length, is predicted for the surviving primordial J/ψ . The ALICE and CMS Collaborations have measured a positive elliptic flow of D mesons in Pb-Pb collisions at $\sqrt{s_{NN}} = 5.02$ TeV [22,23]. The comparison of J/ψ and D meson v_2 could help to constrain the dynamics of charm quarks in the medium and the theoretical model calculations [24–26].

At RHIC, the STAR Collaboration measured, in Au-Au collisions at $\sqrt{s_{NN}} = 200$ GeV, a J/ψ v_2 consistent with zero, albeit with large uncertainties [27]. At the LHC, a first indication of positive J/ψ v_2 was observed by the ALICE Collaboration in semicentral Pb-Pb collisions at $\sqrt{s_{NN}} = 2.76$ TeV with a 2.7σ significance for inclusive J/ψ with $2 < p_T < 6$ GeV/ c at forward rapidity [28]. The CMS Collaboration also reported a positive v_2 for prompt J/ψ at high p_T and midrapidity [29]. A precision measurement of the J/ψ v_2 in Pb-Pb collisions at the highest LHC energy will provide valuable insights on the J/ψ production mechanisms and on the thermalization of charm quarks. Indeed, the higher energy density of the medium should favor charm quark thermalization and, thus, increase its flow. In addition, the larger number of produced $c\bar{c}$ pairs should increase the fraction of J/ψ formed by regeneration mechanisms, both leading to an increase of the observed J/ψ v_2 .

In this Letter, we report ALICE results on inclusive J/ψ elliptic flow in Pb-Pb collisions at $\sqrt{s_{NN}} = 5.02$ TeV for two rapidity ranges. At forward rapidity ($2.5 < y < 4.0$) the J/ψ are measured via the $\mu^+\mu^-$ decay channel and at midrapidity ($|y| < 0.9$) via the e^+e^- decay channel. The results are presented as a function of p_T in the range $0 < p_T < 12$ GeV/ c . For the dimuon channel, different collision centralities are also investigated.

The ALICE detector is described in Ref. [30]. At forward rapidity, the production of quarkonia is measured with the muon spectrometer consisting of a front absorber stopping the hadrons followed by five tracking stations comprising two planes of cathode pad chambers each, with the third station inside a dipole magnet. (In the ALICE reference frame, the muon spectrometer covers a negative η range and consequently a negative y range. We have chosen to present our results with a positive y notation, due to the symmetry of the collision system.) The tracking apparatus is completed by a triggering system made of four planes of resistive plate chambers downstream of an iron wall. At midrapidity, quarkonium production is measured with the central barrel detectors [31]. Tracking within $|\eta| < 0.9$ is performed by the inner tracking system (ITS) [32] and the time projection chamber (TPC) [33]. The specific ionization energy loss (dE/dx) in the gas of the TPC is used for

particle identification (PID). In addition, the silicon pixel detector (SPD) is used to locate the interaction point. The SPD corresponds to the two innermost layers of the ITS covering, respectively, $|\eta| < 2.0$ and $|\eta| < 1.4$. The V0 counters [34], consisting of two arrays of 32 scintillator sectors each covering $2.8 \leq \eta \leq 5.1$ (V0-A) and $-3.7 \leq \eta \leq -1.7$ (V0-C), are used as trigger and centrality detectors [35,36]. As described later, the SPD, TPC, V0-A, and V0-C are also used as event plane detectors. All of these detectors have full azimuthal coverage.

The data were collected in 2015. The analysis at midrapidity uses minimum bias (MB) Pb-Pb collisions. The MB trigger requires a signal in both V0-A and V0-C and is fully efficient for the centrality range 0–90%. At forward rapidity, the analysis uses opposite-sign dimuon (MU) triggered Pb-Pb collisions. The MU trigger requires a MB trigger and at least a pair of opposite-sign track segments in the muon trigger system, each with a p_T above the threshold of the on-line trigger algorithm, set to provide 50% efficiency for muon tracks with $p_T = 1$ GeV/ c . The beam-induced background was further reduced offline using the V0 and the zero degree calorimeter (ZDC) timing information. The contribution from electromagnetic processes was removed by requiring a minimum energy deposited in the neutron ZDCs [37]. The resulting data samples correspond to integrated luminosities of about 13 and 225 μb^{-1} at mid- and forward rapidity, respectively.

J/ψ candidates are formed by combining pairs of opposite-sign tracks reconstructed in the geometrical acceptance of the muon spectrometer or central barrel. The reconstructed tracks in the muon tracker are required to match a track segment in the muon trigger system above the aforementioned p_T threshold. At midrapidity, the tracks must pass a p_T cut of 1 GeV/ c and an electron selection criterion based on the expected dE/dx [33].

The dimuon v_2 is calculated using event plane (EP) based methods. The angle of the reaction plane of the collision is estimated, event by event, by the second-harmonic EP angle Ψ [38], which is obtained from the azimuthal distribution of reconstructed tracks in the TPC or track segments in the SPD for the mid- and forward rapidity analyses, respectively. Effects of nonuniform acceptance in the EP determination are corrected using the methods described in Ref. [39]. At midrapidity, the EP was calculated for each electron pair subtracting the contribution of the pair tracks to remove autocorrelations.

The J/ψ p_T results were obtained, as proposed in Ref. [40], by fitting the distribution of $v_2 = \langle \cos 2(\varphi - \Psi) \rangle$ versus the invariant mass ($m_{\ell\ell}$) of the dilepton pair, with φ being its azimuthal angle. The total flow $v_2(m_{\ell\ell})$ is the combination of the signal and the background flow and can be expressed as

$$v_2(m_{\ell\ell}) = v_2^{\text{sig}} \alpha(m_{\ell\ell}) + v_2^{\text{bkg}}(m_{\ell\ell}) [1 - \alpha(m_{\ell\ell})], \quad (1)$$

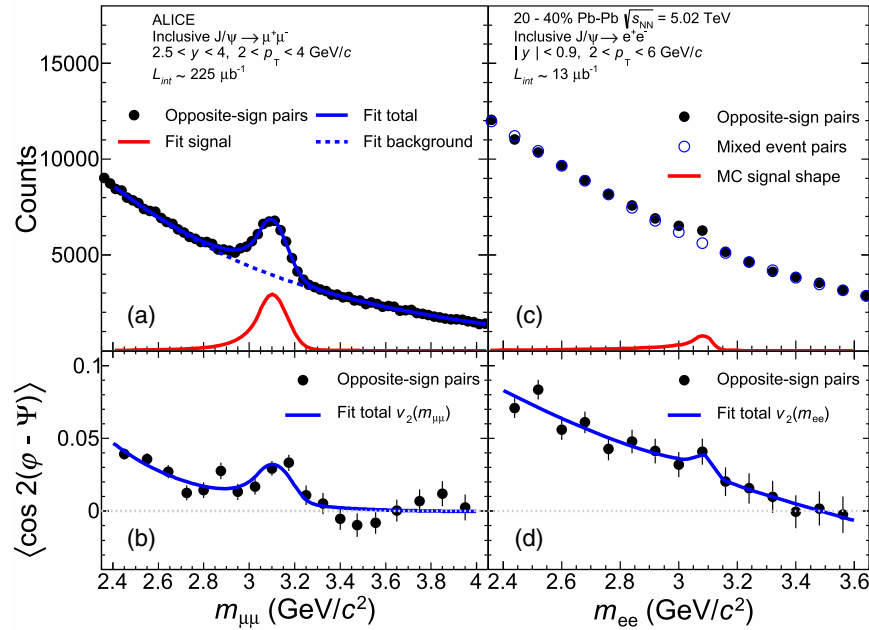


FIG. 1. Invariant mass distribution (top) and $\langle \cos 2(\varphi - \Psi) \rangle$ as a function of $m_{\ell\ell}$ (bottom) of opposite-sign dimuons (left) with $2 < p_T < 4$ GeV/c and $2.5 < y < 4$ and dielectrons (right) with $2 < p_T < 6$ GeV/c and $|y| < 0.9$, in semicentral (20%–40%) Pb-Pb collisions.

where v_2^{sig} and v_2^{bkg} are the elliptic flow of the J/ψ signal (S) and of the background (B), respectively (see the bottom panels in Fig. 1). The signal fraction $\alpha(m_{\ell\ell}) = S(m_{\ell\ell})/[S(m_{\ell\ell}) + B(m_{\ell\ell})]$ was extracted from fits to the invariant mass distribution (see the top panels in Fig. 1) in each p_T and centrality class.

At forward rapidity, the J/ψ peak [S term of $\alpha(m_{\ell\ell})$] is fit with an extended Crystal Ball function or a pseudo-Gaussian, both composed of a Gaussian core with non-Gaussian tails [41]. The underlying continuum [B term of $\alpha(m_{\ell\ell})$] is described with the ratio of second- to third-order polynomials, a pseudo-Gaussian with a width quadratically varying with the mass, or Chebyshev polynomials of the order of six. The background flow v_2^{bkg} was parametrized using a second-order polynomial, a Chebyshev polynomial of the order of four, or the product of a first-order polynomial and an exponential function. At midrapidity, the underlying continuum was estimated combining opposite-sign electrons from different events (using an event-mixing technique) or combining same-sign electrons from the same event. After removing the underlying continuum, the J/ψ signal was obtained by counting the number of dielectrons or from a fit with a Monte Carlo generated shape. The background flow was parametrized using a second-, third-, or fifth-order polynomial depending on the p_T class. Additionally, the PID and track-quality selection criteria were varied as part of the systematic uncertainty evaluation.

The J/ψ v_2 and its statistical uncertainty in each p_T and centrality class were determined as the average of the v_2^{sig}

obtained by fitting $v_2(m_{\ell\ell})$ using Eq. (1) with the various $\alpha(m_{\ell\ell})$ and $v_2^{\text{bkg}}(m_{\ell\ell})$ parametrizations in several invariant mass ranges, while the corresponding systematic uncertainties were defined as the rms of these results. A similar method was used to extract the uncorrected (for detector acceptance and efficiency) average transverse momentum of the reconstructed J/ψ in each centrality and p_T class, which is used to locate the data points when plotted as a function of p_T . Consistent v_2 values were obtained using an alternative method [38], in which the J/ψ raw yield is extracted, as described before, in bins of $(\varphi - \Psi)$ and p_T is evaluated by fitting the data with the function $[dN/d(\varphi - \Psi)] = A[1 + 2v_2 \cos 2(\varphi - \Psi)]$, where A is a normalization constant.

Nonflow effects (J/ψ -EP correlations not related to the initial geometry symmetry plane, such as higher-mass particle decays or jets) were estimated to be small with respect to the other uncertainties by repeating the analysis at forward rapidity using the EP determined in either the V0-A ($\Delta\eta = 5.3$) or the V0-C (no η gap) detector.

The finite resolution in the EP determination smears out the azimuthal distributions and lowers the value of the measured anisotropy [38]. The SPD- and TPC-based EP resolutions were determined by applying the three-subevent method [38]. For the SPD (TPC), the three subevents were obtained using V0-A, V0-C, and SPD, with $\Delta\eta_{\text{V0A-SPD}} = 1.4$ ($\Delta\eta_{\text{V0A-TPC}} = 1.9$), $\Delta\eta_{\text{V0A-V0C}} = 4.5$, and $\Delta\eta_{\text{SPD-V0C}} = 0.3$ ($\Delta\eta_{\text{TPC-V0C}} = 0.8$) pseudorapidity gaps. A systematic uncertainty of 1% on the EP determination was estimated exploiting the availability of different subevents, built from the multiplicity measurement in the

TABLE I. Average number of participants $\langle N_{\text{part}} \rangle$ and SPD EP resolution for each centrality class (expressed in percentage of the nuclear cross section) [36]. The quoted uncertainties are systematic.

Centrality	$\langle N_{\text{part}} \rangle$	EP resolution
5%–20%	287 ± 4	0.873 ± 0.009
20%–40%	160 ± 3	0.910 ± 0.009
40%–60%	70 ± 2	0.832 ± 0.008

V0-A or V0-C, track segments in the SPD, and tracks in the TPC. The EP resolution for each wide centrality class was calculated as the average of the values obtained in finer classes weighted by the number of reconstructed J/ψ . Table I shows the corresponding resolution for each centrality class, applied to the forward rapidity results. For the midrapidity result, the TPC EP resolution is 0.880 ± 0.009 (syst) in the centrality class 20%–40%.

At forward rapidity, the J/ψ reconstruction efficiency depends on the detector occupancy, which could bias the v_2 measurement. This effect was evaluated by embedding azimuthally isotropic simulated decays into real events. The resulting v_2 does not deviate from zero by more than 0.006 in the centrality and p_T classes considered. This value is used as a conservative systematic uncertainty on all measured v_2 values.

Figure 2 shows J/ψ $v_2(p_T)$ at forward and midrapidity in semicentral (20%–40%) Pb-Pb collisions at $\sqrt{s_{NN}} = 5.02$ TeV. The p_T ranges are 0–2, 2–4, 4–6, 6–8, and 8–12 GeV/c and 0–2, 2–6, and 4–12 GeV/c at forward and midrapidity, respectively. The vertical bars indicate the statistical uncertainties, while the boxes indicate the uncorrelated systematic uncertainties. The global relative systematic uncertainty on the EP resolution is 1.0% and is

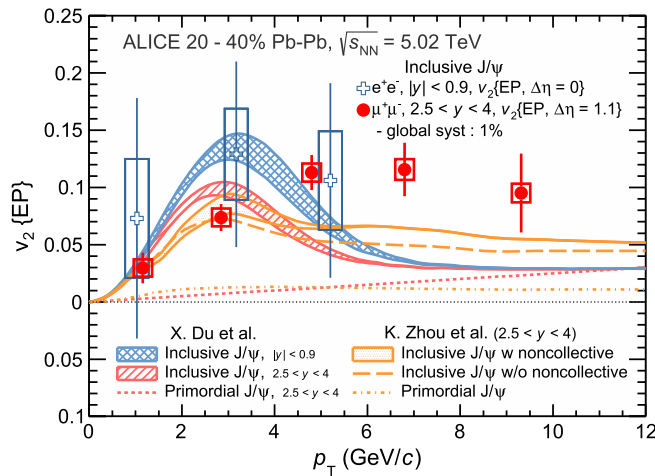


FIG. 2. Inclusive J/ψ $v_2(p_T)$ at forward and midrapidity for semicentral (20%–40%) Pb-Pb collisions at $\sqrt{s_{NN}} = 5.02$ TeV. Calculations from transports model by Refs. [8,25] are also shown.

correlated with p_T . At forward rapidity, a positive v_2 is observed for semicentral collisions (20%–40%). Including statistical and systematic uncertainties, the significance of a nonzero v_2 is as large as 6.6σ in the p_T class 4–6 GeV/c. The J/ψ v_2 increases with p_T up to $v_2 = 0.113 \pm 0.015(\text{stat}) \pm 0.008(\text{syst})$ at $4 < p_T < 6$ GeV/c. The J/ψ $v_2(p_T)$ at midrapidity is similar to that at forward rapidity, albeit with large uncertainties. At midrapidity, the J/ψ v_2 in the range $2 < p_T < 6$ GeV/c is $v_2 = 0.129 \pm 0.080(\text{stat}) \pm 0.040(\text{syst})$.

Transport model calculations including a large J/ψ (re) generation component (about 50% for semicentral collisions) from deconfined charm quarks in the medium [8,25,42] are also shown in Fig. 2. In the model by Du and Rapp [25] (TM1), the v_2 of inclusive J/ψ (hashed and double-hashed bands at forward and midrapidity, respectively) has three origins. First, thermalized charm quarks in the medium transfer a significant elliptic flow to (re) generated J/ψ . Second, primordial J/ψ traverse a longer path through the medium when emitted out of plane than in plane, resulting in a small apparent v_2 (pair dissociation by interactions with the surrounding color charges). Third, when the b quarks thermalize, their flow will be transferred to b hadrons at hadronization and to nonprompt J/ψ from the b -hadron decay. The second component (survival probability of primordial J/ψ) is represented as a short-dashed line to highlight the small J/ψ v_2 in the absence of heavy-quark collective flow. The model by Zhou *et al.* [8] (TM2) includes an additional noncollective J/ψ v_2 component, which arises from the modification of the quarkonium production in the presence of a strong magnetic field in the early stage of the heavy-ion collision [43]. The calculations of TM2 are shown at forward rapidity with (shaded band) and without (long-dashed line) the noncollective J/ψ v_2 component. As for TM1, the v_2 resulting from the different in-plane than out-of-plane survival probability of primordial J/ψ is shown as a dash-dotted line.

TM1 [25] is able to describe qualitatively the J/ψ R_{AA} measurements by ALICE reported in Ref. [10]. The model also agrees with ALICE J/ψ v_2 measurements at forward rapidity at $\sqrt{s_{NN}} = 2.76$ TeV [28] and at midrapidity at $\sqrt{s_{NN}} = 5.02$ TeV. However, at high p_T ($p_T > 4$ GeV/c), clear discrepancies are observed between the model and the J/ψ v_2 at forward rapidity and $\sqrt{s_{NN}} = 5.02$ TeV. Some tension is also seen between the calculations of this model and the R_{AA} measurement by ALICE in this higher p_T range in Ref. [10]. At lower p_T , the model reproduces the magnitude of the measurement by a dominant contribution of J/ψ elliptic flow inherited from thermalized charm quarks. However, the overall shape of the $v_2(p_T)$ is missed, and the v_2 at high p_T is underestimated. This disagreement suggests a missing mechanism in the model. Similar conclusions can be derived from the comparison to TM2 [8]. The addition of the v_2 arising from a possible strong magnetic field in the early stage of heavy-ion collisions

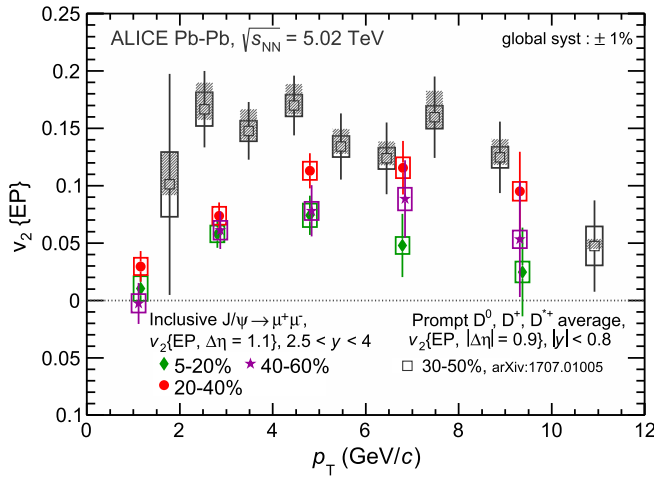


FIG. 3. Inclusive J/ψ $v_2(p_T)$ at forward rapidity in Pb-Pb collisions at $\sqrt{s_{NN}} = 5.02$ TeV for three centrality classes: 5%–20%, 20%–40%, and 40%–60%. The average of D^0 , D^+ , and D^{*+} $v_2(p_T)$ at mid- y in the centrality class 30%–50% is also shown for comparison [22].

[43] improves the comparison with the measured J/ψ v_2 at forward rapidity, especially at high p_T . Such a noncollective component was able to reproduce the prompt J/ψ v_2 at high p_T measured by CMS in Pb-Pb collisions at $\sqrt{s_{NN}} = 2.76$ TeV [29].

Figure 3 presents the p_T dependence of the J/ψ v_2 at forward rapidity for three centrality classes, 5%–20%, 20%–40%, and 40%–60%. As in semicentral (20%–40%) collisions, a significant v_2 is also observed for J/ψ with $2 < p_T < 8$ GeV/ c in the 5%–20% and 40%–60% centrality classes. The p_T dependence of the J/ψ v_2 at forward rapidity is consistent within uncertainties in the three centrality classes presented here. The J/ψ $v_2(p_T)$ appears to be maximum for the 20%–40% centrality class and tends to decrease for more central or peripheral collisions. Interestingly, for identified light hadrons in Pb-Pb collisions at $\sqrt{s_{NN}} = 2.76$ TeV, the $v_2(p_T)$ is maximum in the 40%–60% centrality class and decreases for more central collisions [44]. This different behavior could be understood in the framework of transport models by the increasing contribution of J/ψ regeneration for more central collisions [25,42].

Also shown in Fig. 3 is the $v_2(p_T)$ of prompt D mesons in Pb-Pb collisions at $\sqrt{s_{NN}} = 5.02$ TeV for the 30%–50% centrality class measured by ALICE at midrapidity [22]. The vertical bars indicate the statistical uncertainties, the open boxes the uncorrelated systematic uncertainties, and the shaded boxes the feed-down uncertainties. Although the centrality and rapidity ranges are different, it is clear that at low p_T ($p_T < 4$ GeV/ c) the v_2 of D mesons is higher than that of J/ψ mesons. The large values of the measured v_2 of both D and J/ψ mesons support the conclusion that both D and J/ψ mesons inherit their flow from thermalized charm quarks.

In summary, we report the ALICE measurements of inclusive J/ψ elliptic flow at forward and midrapidity in Pb-Pb collisions at $\sqrt{s_{NN}} = 5.02$ TeV. At forward rapidity, the p_T dependence of the J/ψ v_2 was measured in the 5%–20%, 20%–40%, and 40%–60% centrality classes for $p_T < 12$ GeV/ c . For all the reported centrality classes, a significant J/ψ v_2 signal is observed in the intermediate region $2 < p_T < 8$ GeV/ c . The results unambiguously establish for the first time that J/ψ mesons exhibit collective flow. At midrapidity, the p_T dependence of the J/ψ v_2 was measured in semicentral 20%–40% collisions and is found to be similar to the measurement at forward rapidity, albeit with larger uncertainties. At high p_T , transport models underestimate the measured J/ψ v_2 . The origin of such a discrepancy is currently not understood and suggests a missing mechanism in the models. At low p_T , the magnitude of the observed v_2 is achieved within transport models implementing a strong J/ψ (re)generation component from the (re)combination of thermalized charm quarks in the QGP. Thus, the measurement of the J/ψ elliptic flow combined with the R_{AA} provides substantial evidence for thermalized charm quarks and (re)generation of J/ψ .

The ALICE Collaboration thanks all its engineers and technicians for their invaluable contributions to the construction of the experiment and the CERN accelerator teams for the outstanding performance of the LHC complex. The ALICE Collaboration gratefully acknowledges the resources and support provided by all Grid centres and the Worldwide LHC Computing Grid (WLCG) collaboration. The ALICE Collaboration acknowledges the following funding agencies for their support in building and running the ALICE detector: A.I. Alikhanyan National Science Laboratory (Yerevan Physics Institute) Foundation (ANSL), State Committee of Science and World Federation of Scientists (WFS), Armenia; Austrian Academy of Sciences and Nationalstiftung für Forschung, Technologie und Entwicklung, Austria; Ministry of Communications and High Technologies, National Nuclear Research Center, Azerbaijan; Conselho Nacional de Desenvolvimento Científico e Tecnológico (CNPq), Universidade Federal do Rio Grande do Sul (UFRGS), Financiadora de Estudos e Projetos (Finep) and Fundação de Amparo à Pesquisa do Estado de São Paulo (FAPESP), Brazil; Ministry of Science and Technology of China (MSTC), National Natural Science Foundation of China (NSFC), and Ministry of Education of China (MOEC), China; Ministry of Science, Education and Sport and Croatian Science Foundation, Croatia; Ministry of Education, Youth and Sports of the Czech Republic, Czech Republic; The Danish Council for Independent Research–Natural Sciences, the Carlsberg Foundation, and Danish National Research Foundation (DNRF), Denmark; Helsinki Institute of Physics (HIP), Finland; Commissariat à l’Energie Atomique (CEA) and Institut

National de Physique Nucléaire et de Physique des Particules (IN2P3) and Centre National de la Recherche Scientifique (CNRS), France; Bundesministerium für Bildung, Wissenschaft, Forschung und Technologie (BMBF) and GSI Helmholtzzentrum für Schwerionenforschung GmbH, Germany; General Secretariat for Research and Technology, Ministry of Education, Research and Religions, Greece; National Research, Development and Innovation Office, Hungary; Department of Atomic Energy Government of India (DAE), Department of Science and Technology, Government of India (DST), University Grants Commission, Government of India (UGC) and Council of Scientific and Industrial Research (CSIR), India; Indonesian Institute of Science, Indonesia; Centro Fermi–Museo Storico della Fisica e Centro Studi e Ricerche Enrico Fermi and Istituto Nazionale di Fisica Nucleare (INFN), Italy; Institute for Innovative Science and Technology, Nagasaki Institute of Applied Science (IIST), Japan Society for the Promotion of Science (JSPS) KAKENHI, and Japanese Ministry of Education, Culture, Sports, Science and Technology (MEXT), Japan; Consejo Nacional de Ciencia (CONACYT) y Tecnología, through Fondo de Cooperación Internacional en Ciencia y Tecnología (FONCICYT) and Dirección General de Asuntos del Personal Académico (DGAPA), Mexico; Nederlandse Organisatie voor Wetenschappelijk Onderzoek (NWO), Netherlands; The Research Council of Norway, Norway; Commission on Science and Technology for Sustainable Development in the South (COMSATS), Pakistan; Pontificia Universidad Católica del Perú, Peru; Ministry of Science and Higher Education and National Science Centre, Poland; Korea Institute of Science and Technology Information and National Research Foundation of Korea (NRF), Republic of Korea; Ministry of Education and Scientific Research, Institute of Atomic Physics, and Romanian National Agency for Science, Technology and Innovation, Romania; Joint Institute for Nuclear Research (JINR), Ministry of Education and Science of the Russian Federation, and National Research Centre Kurchatov Institute, Russia; Ministry of Education, Science, Research and Sport of the Slovak Republic, Slovakia; National Research Foundation of South Africa, South Africa; Centro de Aplicaciones Tecnológicas y Desarrollo Nuclear (CEADEN), Cubaenergía, Cuba, Ministerio de Ciencia e Innovación and Centro de Investigaciones Energéticas, Medioambientales y Tecnológicas (CIEMAT), Spain; Swedish Research Council (VR) and Knut and Alice Wallenberg Foundation (KAW), Sweden; European Organization for Nuclear Research, Switzerland; National Science and Technology Development Agency (NSDTA), Suranaree University of Technology (SUT), and Office of the Higher Education Commission under NRU project of Thailand, Thailand; Turkish Atomic Energy

Agency (TAEK), Turkey; National Academy of Sciences of Ukraine, Ukraine; Science and Technology Facilities Council (STFC), United Kingdom; National Science Foundation of the United States of America (NSF) and United States Department of Energy, Office of Nuclear Physics (DOE NP), United States of America.

-
- [1] J. D. Bjorken, Highly relativistic nucleus-nucleus collisions: The central rapidity region, *Phys. Rev. D* **27**, 140 (1983).
 - [2] Y. Aoki, G. Endrodi, Z. Fodor, S. D. Katz, and K. K. Szabo, The order of the quantum chromodynamics transition predicted by the standard model of particle physics, *Nature (London)* **443**, 675 (2006).
 - [3] A. Andronic *et al.*, Heavy-flavour and quarkonium production in the LHC era: From proton-proton to heavy-ion collisions, *Eur. Phys. J. C* **76**, 107 (2016).
 - [4] T. Matsui and H. Satz, J/ψ suppression by quark-gluon plasma formation, *Phys. Lett. B* **178**, 416 (1986).
 - [5] S. Digal, P. Petreczky, and H. Satz, Quarkonium feed down and sequential suppression, *Phys. Rev. D* **64**, 094015 (2001).
 - [6] E. G. Ferreira, Charmonium dissociation and recombination at LHC: Revisiting comovers, *Phys. Lett. B* **731**, 57 (2014).
 - [7] X. Zhao and R. Rapp, Medium modifications and production of charmonia at LHC, *Nucl. Phys. A* **859**, 114 (2011).
 - [8] K. Zhou, N. Xu, Z. Xu, and P. Zhuang, Medium effects on charmonium production at ultrarelativistic energies available at the CERN Large Hadron Collider, *Phys. Rev. C* **89**, 054911 (2014).
 - [9] B. Abelev *et al.* (ALICE Collaboration), J/ψ Suppression at Forward Rapidity in Pb-Pb Collisions at $\sqrt{s_{NN}} = 2.76$ TeV, *Phys. Rev. Lett.* **109**, 072301 (2012).
 - [10] J. Adam *et al.* (ALICE Collaboration), J/ψ suppression at forward rapidity in Pb-Pb collisions at $\sqrt{s_{NN}} = 5.02$ TeV, *Phys. Lett. B* **766**, 212 (2017).
 - [11] A. Adare *et al.* (PHENIX Collaboration), J/ψ Production vs Centrality, Transverse Momentum, and Rapidity in Au + Au Collisions at $\sqrt{s_{NN}} = 200$ GeV, *Phys. Rev. Lett.* **98**, 232301 (2007).
 - [12] A. Adare *et al.* (PHENIX Collaboration), J/ψ suppression at forward rapidity in Au + Au collisions at $\sqrt{s_{NN}} = 200$ GeV, *Phys. Rev. C* **84**, 054912 (2011).
 - [13] L. Adamczyk *et al.* (STAR Collaboration), J/ψ production at low p_T in Au + Au and Cu + Cu collisions at $\sqrt{s_{NN}} = 200$ GeV with the STAR detector, *Phys. Rev. C* **90**, 024906 (2014).
 - [14] L. Adamczyk *et al.* (STAR Collaboration), Energy dependence of J/ψ production in Au + Au collisions at $\sqrt{s_{NN}} = 39, 62.4$ and 200 GeV, *Phys. Lett. B* **771**, 13 (2017).
 - [15] J. Adam *et al.* (ALICE Collaboration), Differential studies of inclusive J/ψ and $\psi(2S)$ production at forward rapidity in Pb-Pb collisions at $\sqrt{s_{NN}} = 2.76$ TeV, *J. High Energy Phys.* **05** (2016) 179.
 - [16] B. B. Abelev *et al.* (ALICE Collaboration), Centrality, rapidity and transverse momentum dependence of J/ψ

- suppression in Pb-Pb collisions at $\sqrt{s_{NN}} = 2.76$ TeV, *Phys. Lett. B* **734**, 314 (2014).
- [17] P. Braun-Munzinger and J. Stachel, (Non)thermal aspects of charmonium production and a new look at J/ψ suppression, *Phys. Lett. B* **490**, 196 (2000).
- [18] A. Andronic, P. Braun-Munzinger, K. Redlich, and J. Stachel, The thermal model on the verge of the ultimate test: Particle production in Pb-Pb collisions at the LHC, *J. Phys. G* **38**, 124081 (2011).
- [19] Y.-p. Liu, Z. Qu, N. Xu, and P.-f. Zhuang, J/ψ transverse momentum distribution in high energy nuclear collisions at RHIC, *Phys. Lett. B* **678**, 72 (2009).
- [20] Y. Liu, N. Xu, and P. Zhuang, J/ψ elliptic flow in relativistic heavy ion collisions, *Nucl. Phys. A* **834**, 317c (2010); (private communication).
- [21] J.-Y. Ollitrault, Anisotropy as a signature of transverse collective flow, *Phys. Rev. D* **46**, 229 (1992).
- [22] S. Acharya *et al.* (ALICE Collaboration), D-meson azimuthal anisotropy in mid-central Pb-Pb collisions at $\sqrt{s_{NN}} = 5.02$ TeV, [arXiv:1707.01005](https://arxiv.org/abs/1707.01005).
- [23] A. M. Sirunyan *et al.* (CMS Collaboration), Measurement of prompt D^0 meson azimuthal anisotropy in PbPb collisions at $\sqrt{s_{NN}} = 5.02$ TeV, [arXiv:1708.03497](https://arxiv.org/abs/1708.03497).
- [24] M. He, R. J. Fries, and R. Rapp, Heavy flavor at the Large Hadron Collider in a strong coupling approach, *Phys. Lett. B* **735**, 445 (2014).
- [25] X. Du and R. Rapp, Sequential regeneration of charmonia in heavy-ion collisions, *Nucl. Phys. A* **943**, 147 (2015).
- [26] Z.-w. Lin and D. Molnar, Quark coalescence and elliptic flow of charm hadrons, *Phys. Rev. C* **68**, 044901 (2003).
- [27] L. Adamczyk *et al.* (STAR Collaboration), Measurement of J/ψ Azimuthal Anisotropy in Au + Au Collisions at $\sqrt{s_{NN}} = 200$ GeV, *Phys. Rev. Lett.* **111**, 052301 (2013).
- [28] E. Abbas *et al.* (ALICE Collaboration), J/ψ Elliptic Flow in Pb-Pb Collisions at $\sqrt{s_{NN}} = 2.76$ TeV, *Phys. Rev. Lett.* **111**, 162301 (2013).
- [29] V. Khachatryan *et al.* (CMS Collaboration), Suppression and azimuthal anisotropy of prompt and nonprompt J/ψ production in Pb-Pb collisions at $\sqrt{s_{NN}} = 2.76$ TeV, *Eur. Phys. J. C* **77**, 252 (2017).
- [30] K. Aamodt *et al.* (ALICE Collaboration), The ALICE experiment at the CERN LHC, *J. Instrum.* **3**, S08002 (2008).
- [31] B. Abelev *et al.* (ALICE Collaboration), Inclusive J/ψ production in pp collisions at $\sqrt{s} = 2.76$ TeV, *Phys. Lett. B* **718**, 295 (2012); Corrigendum, *Phys. Lett. B* **748**, 472(E) (2015).
- [32] K. Aamodt *et al.* (ALICE Collaboration), Alignment of the ALICE Inner Tracking System with cosmic-ray tracks, *J. Instrum.* **5**, P03003 (2010).
- [33] J. Alme *et al.*, The ALICE TPC, a large 3-dimensional tracking device with fast readout for ultra-high multiplicity events, *Nucl. Instrum. Methods Phys. Res., Sect. A* **622**, 316 (2010).
- [34] E. Abbas *et al.* (ALICE Collaboration), Performance of the ALICE VZERO system, *J. Instrum.* **8**, P10016 (2013).
- [35] B. Abelev *et al.* (ALICE Collaboration), Centrality determination of Pb-Pb collisions at $\sqrt{s_{NN}} = 2.76$ TeV with ALICE, *Phys. Rev. C* **88**, 044909 (2013).
- [36] J. Adam *et al.* (ALICE Collaboration), Centrality Dependence of the Charged-Particle Multiplicity Density at Midrapidity in Pb-Pb Collisions at $\sqrt{s_{NN}} = 5.02$ TeV, *Phys. Rev. Lett.* **116**, 222302 (2016).
- [37] B. Abelev *et al.* (ALICE Collaboration), Measurement of the Cross Section for Electromagnetic Dissociation with Neutron Emission in Pb-Pb Collisions at $\sqrt{s_{NN}} = 2.76$ TeV, *Phys. Rev. Lett.* **109**, 252302 (2012).
- [38] A. M. Poskanzer and S. A. Voloshin, Methods for analyzing anisotropic flow in relativistic nuclear collisions, *Phys. Rev. C* **58**, 1671 (1998).
- [39] I. Selyuzhenkov and S. Voloshin, Effects of non-uniform acceptance in anisotropic flow measurement, *Phys. Rev. C* **77**, 034904 (2008).
- [40] N. Borghini and J. Y. Ollitrault, Azimuthally sensitive correlations in nucleus-nucleus collisions, *Phys. Rev. C* **70**, 064905 (2004).
- [41] ALICE Collaboration, Report No. ALICE-PUBLIC-2015-006, 2015, <https://cds.cern.ch/record/2060096>.
- [42] X. Zhao, A. Emerick, and R. Rapp, In-medium quarkonia at SPS, RHIC and LHC, *Nucl. Phys. A* **904–905**, 611c (2013).
- [43] X. Guo, S. Shi, N. Xu, Z. Xu, and P. Zhuang, Magnetic field effect on charmonium production in high energy nuclear collisions, *Phys. Lett. B* **751**, 215 (2015).
- [44] B. B. Abelev *et al.* (ALICE Collaboration), Elliptic flow of identified hadrons in Pb-Pb collisions at $\sqrt{s_{NN}} = 2.76$ TeV, *J. High Energy Phys.* **06** (2015) 190.

S. Acharya,¹³⁷ D. Adamová,⁹⁴ J. Adolphsson,³⁴ M. M. Aggarwal,⁹⁹ G. Aglieri Rinella,³⁵ M. Agnello,³¹ N. Agrawal,⁴⁸ Z. Ahammed,¹³⁷ S. U. Ahn,⁷⁹ S. Aiola,¹⁴¹ A. Akindinov,⁶⁴ M. Al-Turany,¹⁰⁶ S. N. Alam,¹³⁷ D. S. D. Albuquerque,¹²² D. Aleksandrov,⁹⁰ B. Alessandro,⁵⁸ R. Alfaro Molina,⁷⁴ Y. Ali,¹⁵ A. Alici,^{27,53,12} A. Alkin,³ J. Alme,²² T. Alt,⁷⁰ L. Altenkamper,²² I. Altsybeev,¹³⁶ C. Alves Garcia Prado,¹²¹ C. Andrei,⁸⁷ D. Andreou,³⁵ H. A. Andrews,¹¹⁰ A. Andronic,¹⁰⁶ V. Anguelov,¹⁰⁴ C. Anson,⁹⁷ T. Antičić,¹⁰⁷ F. Antinori,⁵⁶ P. Antonioli,⁵³ R. Anwar,¹²⁴ L. Aphecetche,¹¹⁴ H. Appelshäuser,⁷⁰ S. Arcelli,²⁷ R. Arnaldi,⁵⁸ O. W. Arnold,^{105,36} I. C. Arsene,²¹ M. Arslanodok,¹⁰⁴ B. Audurier,¹¹⁴ A. Augustinus,³⁵ R. Averbeck,¹⁰⁶ M. D. Azmi,¹⁷ A. Badalà,⁵⁵ Y. W. Baek,^{60,78} S. Bagnasco,⁵⁸ R. Bailhache,⁷⁰ R. Bala,¹⁰¹ A. Baldisseri,⁷⁵ M. Ball,⁴⁵ R. C. Baral,^{67,88} A. M. Barbano,²⁶ R. Barbera,²⁸ F. Barile,³³ L. Barioglio,²⁶ G. G. Barnaföldi,¹⁴⁰ L. S. Barnby,⁹³ V. Barret,¹³¹ P. Bartalini,⁷ K. Barth,³⁵ E. Bartsch,⁷⁰ N. Bastid,¹³¹ S. Basu,¹³⁹ G. Batigne,¹¹⁴ B. Batyunya,⁷⁷ P. C. Batzing,²¹ J. L. Bazo Alba,¹¹¹ I. G. Bearden,⁹¹ H. Beck,¹⁰⁴ C. Bedda,⁶³ N. K. Behera,⁶⁰ I. Belikov,¹³³ F. Bellini,^{27,35} H. Bello Martinez,²

R. Bellwied,¹²⁴ L. G. E. Beltran,¹²⁰ V. Belyaev,⁸³ G. Bencedi,¹⁴⁰ S. Beole,²⁶ A. Bercuci,⁸⁷ Y. Berdnikov,⁹⁶ D. Berenyi,¹⁴⁰ R. A. Bertens,¹²⁷ D. Berzano,³⁵ L. Betev,³⁵ A. Bhasin,¹⁰¹ I. R. Bhat,¹⁰¹ B. Bhattacharjee,⁴⁴ J. Bhom,¹¹⁸ A. Bianchi,²⁶ L. Bianchi,¹²⁴ N. Bianchi,⁵¹ C. Bianchin,¹³⁹ J. Bielčík,³⁹ J. Bielčíková,⁹⁴ A. Bilandzic,^{36,105} G. Biro,¹⁴⁰ R. Biswas,⁴ S. Biswas,⁴ J. T. Blair,¹¹⁹ D. Blau,⁹⁰ C. Blume,⁷⁰ G. Boca,¹³⁴ F. Bock,³⁵ A. Bogdanov,⁸³ L. Boldizsár,¹⁴⁰ M. Bombara,⁴⁰ G. Bonomi,¹³⁵ M. Bonora,³⁵ J. Book,⁷⁰ H. Borel,⁷⁵ A. Borisso,^{104,19} M. Borri,¹²⁶ E. Botta,²⁶ C. Bourjau,⁹¹ L. Bratrud,⁷⁰ P. Braun-Munzinger,¹⁰⁶ M. Bregant,¹²¹ T. A. Broker,⁷⁰ M. Broz,³⁹ E. J. Brucken,⁴⁶ E. Bruna,⁵⁸ G. E. Bruno,^{35,33} D. Budnikov,¹⁰⁸ H. Buesching,⁷⁰ S. Bufalino,³¹ P. Buhler,¹¹³ P. Buncic,³⁵ O. Busch,¹³⁰ Z. Buthelezi,⁷⁶ J. B. Butt,¹⁵ J. T. Buxton,¹⁸ J. Cabala,¹¹⁶ D. Caffarri,^{35,92} H. Caines,¹⁴¹ A. Caliva,^{63,106} E. Calvo Villar,¹¹¹ P. Camerini,²⁵ A. A. Capon,¹¹³ F. Carena,³⁵ W. Carena,³⁵ F. Carnesecchi,^{27,12} J. Castillo Castellanos,⁷⁵ A. J. Castro,¹²⁷ E. A. R. Casula,⁵⁴ C. Ceballos Sanchez,⁹ S. Chandra,¹³⁷ B. Chang,¹²⁵ W. Chang,⁷ S. Chapeland,³⁵ M. Chartier,¹²⁶ S. Chattopadhyay,¹³⁷ S. Chattopadhyay,¹⁰⁹ A. Chauvin,^{36,105} C. Cheshkov,¹³² B. Cheynis,¹³² V. Chibante Barroso,³⁵ D. D. Chinellato,¹²² S. Cho,⁶⁰ P. Chochula,³⁵ M. Chojnacki,⁹¹ S. Choudhury,¹³⁷ T. Chowdhury,¹³¹ P. Christakoglou,⁹² C. H. Christensen,⁹¹ P. Christiansen,³⁴ T. Chujo,¹³⁰ S. U. Chung,¹⁹ C. Cicalo,⁵⁴ L. Cifarelli,^{12,27} F. Cindolo,⁵³ J. Cleymans,¹⁰⁰ F. Colamaria,^{52,33} D. Colella,^{35,52,65} A. Collu,⁸² M. Colocci,²⁷ M. Concas,^{58,‡} G. Conesa Balbastre,⁸¹ Z. Conesa del Valle,⁶¹ J. G. Contreras,³⁹ T. M. Cormier,⁹⁵ Y. Corrales Morales,⁵⁸ I. Cortés Maldonado,² P. Cortese,³² M. R. Cosentino,¹²³ F. Costa,³⁵ S. Costanza,¹³⁴ J. Crkovská,⁶¹ P. Crochet,¹³¹ E. Cuautle,⁷² L. Cunqueiro,^{95,71} T. Dahms,^{36,105} A. Dainese,⁵⁶ M. C. Danisch,¹⁰⁴ A. Danu,⁶⁸ D. Das,¹⁰⁹ I. Das,¹⁰⁹ S. Das,⁴ A. Dash,⁸⁸ S. Dash,⁴⁸ S. De,⁴⁹ A. De Caro,³⁰ G. de Cataldo,⁵² C. de Conti,¹²¹ J. de Cuveland,⁴² A. De Falco,²⁴ D. De Gruttola,^{30,12} N. De Marco,⁵⁸ S. De Pasquale,³⁰ R. D. De Souza,¹²² H. F. Degenhardt,¹²¹ A. Deisting,^{106,104} A. Deloff,⁸⁶ C. Deplano,⁹² P. Dhankher,⁴⁸ D. Di Bari,³³ A. Di Mauro,³⁵ P. Di Nezza,⁵¹ B. Di Ruzza,⁵⁶ M. A. Diaz Corchero,¹⁰ T. Dietel,¹⁰⁰ P. Dillenseger,⁷⁰ Y. Ding,⁷ R. Divià,³⁵ Ø. Djuvsland,²² A. Dobrin,³⁵ D. Domenicis Gimenez,¹²¹ B. Dönigus,⁷⁰ O. Dordic,²¹ L. V. R. Doremalen,⁶³ A. K. Dubey,¹³⁷ A. Dubla,¹⁰⁶ L. Ducroux,¹³² S. Dudi,⁹⁹ A. K. Duggal,⁹⁹ M. Dukhishyam,⁸⁸ P. Dupieux,¹³¹ R. J. Ehlers,¹⁴¹ D. Elia,⁵² E. Endress,¹¹¹ H. Engel,⁶⁹ E. Epple,¹⁴¹ B. Erazmus,¹¹⁴ F. Erhardt,⁹⁸ B. Espagnon,⁶¹ G. Eulisse,³⁵ J. Eum,¹⁹ D. Evans,¹¹⁰ S. Evdokimov,¹¹² L. Fabbietti,^{105,36} J. Faivre,⁸¹ A. Fantoni,⁵¹ M. Fasel,⁹⁵ L. Feldkamp,⁷¹ A. Feliciello,⁵⁸ G. Feofilov,¹³⁶ A. Fernández Téllez,² E. G. Ferreira,¹⁶ A. Ferretti,²⁶ A. Festanti,^{29,35} V. J. G. Feuillard,^{75,131} J. Figiel,¹¹⁸ M. A. S. Figueredo,¹²¹ S. Filchagin,¹⁰⁸ D. Finogeev,⁶² F. M. Fionda,^{22,24} M. Floris,³⁵ S. Foertsch,⁷⁶ P. Foka,¹⁰⁶ S. Fokin,⁹⁰ E. Fragiaco,⁵⁹ A. Francescon,³⁵ A. Francisco,¹¹⁴ U. Frankfeld,¹⁰⁶ G. G. Fronze,²⁶ U. Fuchs,³⁵ C. Furget,⁸¹ A. Furs,⁶² M. Fusco Girard,³⁰ J. J. Gaardhøje,⁹¹ M. Gagliardi,²⁶ A. M. Gago,¹¹¹ K. Gajdosova,⁹¹ M. Gallio,²⁶ C. D. Galvan,¹²⁰ P. Ganoti,⁸⁵ C. Garabatos,¹⁰⁶ E. Garcia-Solis,¹³ K. Garg,²⁸ C. Gargiulo,³⁵ P. Gasik,^{105,36} E. F. Gauger,¹¹⁹ M. B. Gay Ducati,⁷³ M. Germain,¹¹⁴ J. Ghosh,¹⁰⁹ P. Ghosh,¹³⁷ S. K. Ghosh,⁴ P. Gianotti,⁵¹ P. Giubellino,^{35,106,58} P. Giubilato,²⁹ E. Gladysz-Dziadus,¹¹⁸ P. Glässel,¹⁰⁴ D. M. Gómez Coral,⁷⁴ A. Gomez Ramirez,⁶⁹ A. S. Gonzalez,³⁵ V. Gonzalez,¹⁰ P. González-Zamora,^{10,2} S. Gorbunov,⁴² L. Görlich,¹¹⁸ S. Gotovac,¹¹⁷ V. Grabski,⁷⁴ L. K. Graczykowski,¹³⁸ K. L. Graham,¹¹⁰ L. Greiner,⁸² A. Grelli,⁶³ C. Grigoras,³⁵ V. Grigoriev,⁸³ A. Grigoryan,¹ S. Grigoryan,⁷⁷ J. M. Gronefeld,¹⁰⁶ F. Grosa,³¹ J. F. Grosse-Oetringhaus,³⁵ R. Grosso,¹⁰⁶ F. Guber,⁶² R. Guernane,⁸¹ B. Guerzoni,²⁷ K. Gulbrandsen,⁹¹ T. Gunji,¹²⁹ A. Gupta,¹⁰¹ R. Gupta,¹⁰¹ I. B. Guzman,² R. Haake,³⁵ C. Hadjidakis,⁶¹ H. Hamagaki,⁸⁴ G. Hamar,¹⁴⁰ J. C. Hamon,¹³³ M. R. Haque,⁶³ J. W. Harris,¹⁴¹ A. Harton,¹³ H. Hassan,⁸¹ D. Hatzifotiadou,^{12,53} S. Hayashi,¹²⁹ S. T. Heckel,⁷⁰ E. Hellbär,⁷⁰ H. Helstrup,³⁷ A. Herghelegiu,⁸⁷ E. G. Hernandez,² G. Herrera Corral,¹¹ F. Herrmann,⁷¹ B. A. Hess,¹⁰³ K. F. Hetland,³⁷ H. Hillemanns,³⁵ C. Hills,¹²⁶ B. Hippolyte,¹³³ B. Hohlweger,¹⁰⁵ D. Horak,³⁹ S. Hornung,¹⁰⁶ R. Hosokawa,^{81,130} P. Hristov,³⁵ C. Hughes,¹²⁷ T. J. Humanic,¹⁸ N. Hussain,⁴⁴ T. Hussain,¹⁷ D. Hutter,⁴² D. S. Hwang,²⁰ S. A. Iga Buitron,⁷² R. Ilkaev,¹⁰⁸ M. Inaba,¹³⁰ M. Ippolitov,^{83,90} M. S. Islam,¹⁰⁹ M. Ivanov,¹⁰⁶ V. Ivanov,⁹⁶ V. Izucheev,¹¹² B. Jacak,⁸² N. Jacazio,²⁷ P. M. Jacobs,⁸² M. B. Jadhav,⁴⁸ S. Jadlovská,¹¹⁶ J. Jadlovsky,¹¹⁶ S. Jaelani,⁶³ C. Jahnke,³⁶ M. J. Jakubowska,¹³⁸ M. A. Janik,¹³⁸ P. H. S. Y. Jayarathna,¹²⁴ C. Jena,⁸⁸ M. Jercic,⁹⁸ R. T. Jimenez Bustamante,¹⁰⁶ P. G. Jones,¹¹⁰ A. Jusko,¹¹⁰ P. Kalinak,⁶⁵ A. Kalweit,³⁵ J. H. Kang,¹⁴² V. Kaplin,⁸³ S. Kar,¹³⁷ A. Karasu Uysal,⁸⁰ O. Karavichev,⁶² T. Karavicheva,⁶² L. Karayan,^{106,104} P. Karczmarczyk,³⁵ E. Karpechev,⁶² U. Kebschull,⁶⁹ R. Keidel,¹⁴³ D. L. D. Keijdener,⁶³ M. Keil,³⁵ B. Ketzer,⁴⁵ Z. Khabanova,⁹² P. Khan,¹⁰⁹ S. A. Khan,¹³⁷ A. Khanzadeev,⁹⁶ Y. Kharlov,¹¹² A. Khatun,¹⁷ A. Khuntia,⁴⁹ M. M. Kielbowicz,¹¹⁸ B. Kileng,³⁷ B. Kim,¹³⁰ D. Kim,¹⁴² D. J. Kim,¹²⁵ H. Kim,¹⁴² J. S. Kim,⁴³ J. Kim,¹⁰⁴ M. Kim,⁶⁰ S. Kim,²⁰ T. Kim,¹⁴² S. Kirsch,⁴² I. Kisel,⁴² S. Kiselev,⁶⁴ A. Kisiel,¹³⁸ G. Kiss,¹⁴⁰ J. L. Klay,⁶ C. Klein,⁷⁰ J. Klein,³⁵ C. Klein-Bösing,⁷¹ S. Klewin,¹⁰⁴ A. Kluge,³⁵ M. L. Knichel,^{104,35} A. G. Knospe,¹²⁴ C. Kobdaj,¹¹⁵ M. Kofarago,¹⁴⁰ M. K. Köhler,¹⁰⁴ T. Kollegger,¹⁰⁶ V. Kondratiev,¹³⁶ N. Kondratyeva,⁸³ E. Kondratyuk,¹¹² A. Konevskikh,⁶²

M. Konyushikhin,¹³⁹ M. Kopicik,¹¹⁶ M. Kour,¹⁰¹ C. Kouzinopoulos,³⁵ O. Kovalenko,⁸⁶ V. Kovalenko,¹³⁶ M. Kowalski,¹¹⁸ G. Koyithatta Meethalevedu,⁴⁸ I. Králík,⁶⁵ A. Kravčáková,⁴⁰ L. Kreis,¹⁰⁶ M. Krivda,^{110,65} F. Krizek,⁹⁴ E. Kryshen,⁹⁶ M. Krzewicki,⁴² A. M. Kubera,¹⁸ V. Kučera,⁹⁴ C. Kuhn,¹³³ P. G. Kuijer,⁹² A. Kumar,¹⁰¹ J. Kumar,⁴⁸ L. Kumar,⁹⁹ S. Kumar,⁴⁸ S. Kundu,⁸⁸ P. Kurashvili,⁸⁶ A. Kurepin,⁶² A. B. Kurepin,⁶² A. Kuryakin,¹⁰⁸ S. Kushpil,⁹⁴ M. J. Kweon,⁶⁰ Y. Kwon,¹⁴² S. L. La Pointe,⁴² P. La Rocca,²⁸ C. Lagana Fernandes,¹²¹ Y. S. Lai,⁸² I. Lakomov,³⁵ R. Langoy,⁴¹ K. Lapidus,¹⁴¹ C. Lara,⁶⁹ A. Lardeux,²¹ A. Lattuca,²⁶ E. Laudi,³⁵ R. Lavicka,³⁹ R. Lea,²⁵ L. Leardini,¹⁰⁴ S. Lee,¹⁴² F. Lehas,⁹² S. Lehner,¹¹³ J. Lehrbach,⁴² R. C. Lemmon,⁹³ E. Leogrande,⁶³ I. León Monzón,¹²⁰ P. Lévai,¹⁴⁰ X. Li,¹⁴ J. Lien,⁴¹ R. Lietava,¹¹⁰ B. Lim,¹⁹ S. Lindal,²¹ V. Lindenstruth,⁴² S. W. Lindsay,¹²⁶ C. Lippmann,¹⁰⁶ M. A. Lisa,¹⁸ V. Litichevskiy,⁴⁶ W. J. Llope,¹³⁹ D. F. Lodato,⁶³ P. I. Loenne,²² V. Loginov,⁸³ C. Loizides,^{95,82} P. Loncar,¹¹⁷ X. Lopez,¹³¹ E. López Torres,⁹ A. Lowe,¹⁴⁰ P. Luettig,⁷⁰ J. R. Luhder,⁷¹ M. Lunardon,²⁹ G. Luparello,^{59,25} M. Lupi,³⁵ T. H. Lutz,¹⁴¹ A. Maevskaya,⁶² M. Mager,³⁵ S. M. Mahmood,²¹ A. Maire,¹³³ R. D. Majka,¹⁴¹ M. Malaev,⁹⁶ L. Malinina,^{77,8} D. Mal'Kevich,⁶⁴ P. Malzacher,¹⁰⁶ A. Mamonov,¹⁰⁸ V. Manko,⁹⁰ F. Manso,¹³¹ V. Manzari,⁵² Y. Mao,⁷ M. Marchisone,^{132,76,128} J. Mareš,⁶⁶ G. V. Margagliotti,²⁵ A. Margotti,⁵³ J. Margutti,⁶³ A. Marín,¹⁰⁶ C. Markert,¹¹⁹ M. Marquard,⁷⁰ N. A. Martin,¹⁰⁶ P. Martinengo,³⁵ J. A. L. Martinez,⁶⁹ M. I. Martínez,² G. Martínez García,¹¹⁴ M. Martinez Pedreira,³⁵ S. Masciocchi,¹⁰⁶ M. Maserà,²⁶ A. Masoni,⁵⁴ E. Masson,¹¹⁴ A. Mastroserio,⁵² A. M. Mathis,^{105,36} P. F. T. Matuoka,¹²¹ A. Matyja,¹²⁷ C. Mayer,¹¹⁸ J. Mazer,¹²⁷ M. Mazzilli,³³ M. A. Mazzoni,⁵⁷ F. Meddi,²³ Y. Melikyan,⁸³ A. Menchaca-Rocha,⁷⁴ E. Meninno,³⁰ J. Mercado Pérez,¹⁰⁴ M. Meres,³⁸ S. Mhlanga,¹⁰⁰ Y. Miake,¹³⁰ M. M. Mieskolainen,⁴⁶ D. L. Mihaylov,¹⁰⁵ K. Mikhaylov,^{64,77} A. Mischke,⁶³ A. N. Mishra,⁴⁹ D. Miśkowiec,¹⁰⁶ J. Mitra,¹³⁷ C. M. Mitu,⁶⁸ N. Mohammadi,⁶³ A. P. Mohanty,⁶³ B. Mohanty,⁸⁸ M. Mohisin Khan,^{17,||} E. Montes,¹⁰ D. A. Moreira De Godoy,⁷¹ L. A. P. Moreno,² S. Moretto,²⁹ A. Morreale,¹¹⁴ A. Morsch,³⁵ V. Muccifora,⁵¹ E. Mudnic,¹¹⁷ D. Mühlheim,⁷¹ S. Muhuri,¹³⁷ M. Mukherjee,⁴ J. D. Mulligan,¹⁴¹ M. G. Munhoz,¹²¹ K. Munning,⁴⁵ R. H. Munzer,⁷⁰ H. Murakami,¹²⁹ S. Murray,⁷⁶ L. Musa,³⁵ J. Musinsky,⁶⁵ C. J. Myers,¹²⁴ J. W. Myrcha,¹³⁸ D. Nag,⁴ B. Naik,⁴⁸ R. Nair,⁸⁶ B. K. Nandi,⁴⁸ R. Nania,^{12,53} E. Nappi,⁵² A. Narayan,⁴⁸ M. U. Naru,¹⁵ H. Natal da Luz,¹²¹ C. Natrass,¹²⁷ S. R. Navarro,² K. Nayak,⁸⁸ R. Nayak,⁴⁸ T. K. Nayak,¹³⁷ S. Nazarenko,¹⁰⁸ R. A. Negrao De Oliveira,³⁵ L. Nellen,⁷² S. V. Nesbo,³⁷ F. Ng,¹²⁴ M. Nicassio,¹⁰⁶ M. Niculescu,⁶⁸ J. Niedziela,^{138,35} B. S. Nielsen,⁹¹ S. Nikolaev,⁹⁰ S. Nikulin,⁹⁰ V. Nikulin,⁹⁶ F. Noferini,^{12,53} P. Nomokonov,⁷⁷ G. Nooren,⁶³ J. C. C. Noris,² J. Norman,¹²⁶ A. Nyanin,⁹⁰ J. Nystrand,²² H. Oeschler,^{104,19,†} A. Ohlson,¹⁰⁴ T. Okubo,⁴⁷ L. Olah,¹⁴⁰ J. Oleniacz,¹³⁸ A. C. Oliveira Da Silva,¹²¹ M. H. Oliver,¹⁴¹ J. Onderwaater,¹⁰⁶ C. Oppedisano,⁵⁸ R. Orava,⁴⁶ M. Oravec,¹¹⁶ A. Ortiz Velasquez,⁷² A. Oskarsson,³⁴ J. Otwinowski,¹¹⁸ K. Oyama,⁸⁴ Y. Pachmayer,¹⁰⁴ V. Pacik,⁹¹ D. Pagano,¹³⁵ G. Paić,⁷² P. Palni,⁷ J. Pan,¹³⁹ A. K. Pandey,⁴⁸ S. Panebianco,⁷⁵ V. Papikyan,¹ P. Pareek,⁴⁹ J. Park,⁶⁰ S. Parmar,⁹⁹ A. Passfeld,⁷¹ S. P. Pathak,¹²⁴ R. N. Patra,¹³⁷ B. Paul,⁵⁸ H. Pei,⁷ T. Peitzmann,⁶³ X. Peng,⁷ L. G. Pereira,⁷³ H. Pereira Da Costa,⁷⁵ D. Peresunko,^{83,90} E. Perez Lezama,⁷⁰ V. Peskov,⁷⁰ Y. Pestov,⁵ V. Petráček,³⁹ V. Petrov,¹¹² M. Petrovici,⁸⁷ C. Petta,²⁸ R. P. Pezzi,⁷³ S. Piano,⁵⁹ M. Pikna,³⁸ P. Pillot,¹¹⁴ L. O. D. L. Pimentel,⁹¹ O. Pinazza,^{53,35} L. Pinsky,¹²⁴ D. B. Piyarathna,¹²⁴ M. Płoskoń,⁸² M. Planinic,⁹⁸ F. Pliquet,⁷⁰ J. Pluta,¹³⁸ S. Pochybova,¹⁴⁰ P. L. M. Podesta-Lerma,¹²⁰ M. G. Poghosyan,⁹⁵ B. Polichtchouk,¹¹² N. Poljak,⁹⁸ W. Poonsawat,¹¹⁵ A. Pop,⁸⁷ H. Poppenborg,⁷¹ S. Porteboeuf-Houssais,¹³¹ V. Pozdniakov,⁷⁷ S. K. Prasad,⁴ R. Preghenella,⁵³ F. Prino,⁵⁸ C. A. Pruneau,¹³⁹ I. Pshenichnov,⁶² M. Puccio,²⁶ V. Punin,¹⁰⁸ J. Putschke,¹³⁹ S. Raha,⁴ S. Rajput,¹⁰¹ J. Rak,¹²⁵ A. Rakotozafindrabe,⁷⁵ L. Ramello,³² F. Rami,¹³³ D. B. Rana,¹²⁴ R. Raniwala,¹⁰² S. Raniwala,¹⁰² S. S. Räsänen,⁴⁶ B. T. Rascanu,⁷⁰ D. Rathee,⁹⁹ V. Ratzka,⁴⁵ I. Ravasenga,³¹ K. F. Read,^{127,95} K. Redlich,^{86,¶} A. Rehman,²² P. Reichelt,⁷⁰ F. Reidt,³⁵ X. Ren,⁷ R. Renfordt,⁷⁰ A. Reshetin,⁶² K. Reygers,¹⁰⁴ V. Riabov,⁹⁶ T. Richert,^{63,34} M. Richter,²¹ P. Riedler,³⁵ W. Riegler,³⁵ F. Riggi,²⁸ C. Ristea,⁶⁸ M. Rodríguez Cahuantzi,² K. Røed,²¹ E. Rogochaya,⁷⁷ D. Rohr,^{35,42} D. Röhrich,²² P. S. Rokita,¹³⁸ F. Ronchetti,⁵¹ E. D. Rosas,⁷² P. Rosnet,¹³¹ A. Rossi,^{29,56} A. Rotondi,¹³⁴ F. Roukoutakis,⁸⁵ C. Roy,¹³³ P. Roy,¹⁰⁹ A. J. Rubio Montero,¹⁰ O. V. Rueda,⁷² R. Rui,²⁵ B. Rumyantsev,⁷⁷ A. Rustamov,⁸⁹ E. Ryabinkin,⁹⁰ Y. Ryabov,⁹⁶ A. Rybicki,¹¹⁸ S. Saarinen,⁴⁶ S. Sadhu,¹³⁷ S. Sadovsky,¹¹² K. Šafařík,³⁵ S. K. Saha,¹³⁷ B. Sahlmuller,⁷⁰ B. Sahoo,⁴⁸ P. Sahoo,⁴⁹ R. Sahoo,⁴⁹ S. Sahoo,⁶⁷ P. K. Sahu,⁶⁷ J. Saini,¹³⁷ S. Sakai,¹³⁰ M. A. Saleh,¹³⁹ J. Salzwedel,¹⁸ S. Sambyal,¹⁰¹ V. Samsonov,^{96,83} A. Sandoval,⁷⁴ A. Sarkar,⁷⁶ D. Sarkar,¹³⁷ N. Sarkar,¹³⁷ P. Sarma,⁴⁴ M. H. P. Sas,⁶³ E. Scapparone,⁵³ F. Scarlassara,²⁹ B. Schaefer,⁹⁵ H. S. Scheid,⁷⁰ C. Schiaua,⁸⁷ R. Schicker,¹⁰⁴ C. Schmidt,¹⁰⁶ H. R. Schmidt,¹⁰³ M. O. Schmidt,¹⁰⁴ M. Schmidt,¹⁰³ N. V. Schmidt,^{70,95} J. Schukraft,³⁵ Y. Schutz,^{35,133} K. Schwarz,¹⁰⁶ K. Schweda,¹⁰⁶ G. Scioli,²⁷ E. Scomparin,⁵⁸ M. Šefčík,⁴⁰ J. E. Seger,⁹⁷ Y. Sekiguchi,¹²⁹ D. Sekihata,⁴⁷ I. Selyuzhenkov,^{106,83} K. Senosi,⁷⁶ S. Senyukov,¹³³ E. Serradilla,^{10,74} P. Sett,⁴⁸ A. Sevcenco,⁶⁸ A. Shabanov,⁶² A. Shabetai,¹¹⁴ R. Shahoyan,³⁵ W. Shaikh,¹⁰⁹ A. Shangaraev,¹¹² A. Sharma,⁹⁹ A. Sharma,¹⁰¹ M. Sharma,¹⁰¹ M. Sharma,¹⁰¹ N. Sharma,⁹⁹ A. I. Sheikh,¹³⁷ K. Shigaki,⁴⁷

S. Shirinkin,⁶⁴ Q. Shou,⁷ K. Shtejer,^{9,26} Y. Sibiriak,⁹⁰ S. Siddhanta,⁵⁴ K. M. Sielewicz,³⁵ T. Siemiarczuk,⁸⁶ S. Silaeva,⁹⁰ D. Silvermyr,³⁴ G. Simatovic,⁹² G. Simonetti,³⁵ R. Singaraju,¹³⁷ R. Singh,⁸⁸ V. Singhal,¹³⁷ T. Sinha,¹⁰⁹ B. Sitar,³⁸ M. Sitta,³² T. B. Skaali,²¹ M. Slupecki,¹²⁵ N. Smirnov,¹⁴¹ R. J. M. Snellings,⁶³ T. W. Snellman,¹²⁵ J. Song,¹⁹ M. Song,¹⁴² F. Soramel,²⁹ S. Sorensen,¹²⁷ F. Sozzi,¹⁰⁶ I. Sputowska,¹¹⁸ J. Stachel,¹⁰⁴ I. Stan,⁶⁸ P. Stankus,⁹⁵ E. Stenlund,³⁴ D. Stocco,¹¹⁴ M. M. Stortvedt,³⁷ P. Strmen,³⁸ A. A. P. Suaide,¹²¹ T. Sugitate,⁴⁷ C. Suires,⁶¹ M. Suleymanov,¹⁵ M. Suljic,²⁵ R. Sultanov,⁶⁴ M. Šumbera,⁹⁴ S. Sumowidagdo,⁵⁰ K. Suzuki,¹¹³ S. Swain,⁶⁷ A. Szabo,³⁸ I. Szarka,³⁸ U. Tabassam,¹⁵ J. Takahashi,¹²² G. J. Tambave,²² N. Tanaka,¹³⁰ M. Tarhini,⁶¹ M. Tariq,¹⁷ M. G. Tarzila,⁸⁷ A. Tauro,³⁵ G. Tejada Muñoz,² A. Telesca,³⁵ K. Terasaki,¹²⁹ C. Terrevoli,²⁹ B. Teyssier,¹³² D. Thakur,⁴⁹ S. Thakur,¹³⁷ D. Thomas,¹¹⁹ F. Thoresen,⁹¹ R. Tieulent,¹³² A. Tikhonov,⁶² A. R. Timmins,¹²⁴ A. Toia,⁷⁰ M. Toppi,⁵¹ S. R. Torres,¹²⁰ S. Tripathy,⁴⁹ S. Trogolo,²⁶ G. Trombetta,³³ L. Tropp,⁴⁰ V. Trubnikov,³ W. H. Trzaska,¹²⁵ B. A. Trzeciak,⁶³ T. Tsuji,¹²⁹ A. Tumkin,¹⁰⁸ R. Turrisi,⁵⁶ T. S. Tveter,²¹ K. Ullaland,²² E. N. Umaka,¹²⁴ A. Uras,¹³² G. L. Usai,²⁴ A. Utrobicic,⁹⁸ M. Vala,^{116,65} J. Van Der Maarel,⁶³ J. W. Van Hoorne,³⁵ M. van Leeuwen,⁶³ T. Vanat,⁹⁴ P. Vande Vyvre,³⁵ D. Varga,¹⁴⁰ A. Vargas,² M. Vargyas,¹²⁵ R. Varma,⁴⁸ M. Vasileiou,⁸⁵ A. Vasiliev,⁹⁰ A. Vauthier,⁸¹ O. Vázquez Doce,^{105,36} V. Vechernin,¹³⁶ A. M. Veen,⁶³ A. Velure,²² E. Vercellin,²⁶ S. Vergara Limón,² R. Vernet,⁸ R. Vértesi,¹⁴⁰ L. Vickovic,¹¹⁷ S. Vigolo,⁶³ J. Viinikainen,¹²⁵ Z. Vilakazi,¹²⁸ O. Villalobos Baillie,¹¹⁰ A. Villatoro Tello,² A. Vinogradov,⁹⁰ L. Vinogradov,¹³⁶ T. Virgili,³⁰ V. Vislavicius,³⁴ A. Vodopyanov,⁷⁷ M. A. Völkl,¹⁰³ K. Voloshin,⁶⁴ S. A. Voloshin,¹³⁹ G. Volpe,³³ B. von Haller,³⁵ I. Vorobyev,^{105,36} D. Voscek,¹¹⁶ D. Vranic,^{35,106} J. Vrláková,⁴⁰ B. Wagner,²² H. Wang,⁶³ M. Wang,⁷ D. Watanabe,¹³⁰ Y. Watanabe,^{129,130} M. Weber,¹¹³ S. G. Weber,¹⁰⁶ D. F. Weiser,¹⁰⁴ S. C. Wenzel,³⁵ J. P. Wessels,⁷¹ U. Westerhoff,⁷¹ A. M. Whitehead,¹⁰⁰ J. Wiechula,⁷⁰ J. Wikne,²¹ G. Wilk,⁸⁶ J. Wilkinson,^{104,53} G. A. Willems,^{35,71} M. C. S. Williams,⁵³ E. Willsher,¹¹⁰ B. Windelband,¹⁰⁴ W. E. Witt,¹²⁷ R. Xu,⁷ S. Yalcin,⁸⁰ K. Yamakawa,⁴⁷ P. Yang,⁷ S. Yano,⁴⁷ Z. Yin,⁷ H. Yokoyama,^{130,81} I.-K. Yoo,¹⁹ J. H. Yoon,⁶⁰ E. Yun,¹⁹ V. Yurchenko,³ V. Zaccolo,⁵⁸ A. Zaman,¹⁵ C. Zampolli,³⁵ H. J. C. Zanoli,¹²¹ N. Zardoshti,¹¹⁰ A. Zarochentsev,¹³⁶ P. Závada,⁶⁶ N. Zaviyalov,¹⁰⁸ H. Zbroszczyk,¹³⁸ M. Zhalov,⁹⁶ H. Zhang,^{22,7} X. Zhang,⁷ Y. Zhang,⁷ C. Zhang,⁶³ Z. Zhang,^{7,131} C. Zhao,²¹ N. Zhigareva,⁶⁴ D. Zhou,⁷ Y. Zhou,⁹¹ Z. Zhou,²² H. Zhu,²² J. Zhu,⁷ Y. Zhu,⁷ A. Zichichi,^{12,27} M. B. Zimmermann,³⁵ G. Zinovjev,³ J. Zmeskal,¹¹³ and S. Zou⁷

(ALICE Collaboration)

¹A.I. Alikhanyan National Science Laboratory (Yerevan Physics Institute) Foundation, Yerevan, Armenia²Benemérita Universidad Autónoma de Puebla, Puebla, Mexico³Bogolyubov Institute for Theoretical Physics, Kiev, Ukraine⁴Bose Institute, Department of Physics and Centre for Astroparticle Physics and Space Science (CAPSS), Kolkata, India⁵Budker Institute for Nuclear Physics, Novosibirsk, Russia⁶California Polytechnic State University, San Luis Obispo, California, USA⁷Central China Normal University, Wuhan, China⁸Centre de Calcul de l'IN2P3, Villeurbanne, Lyon, France⁹Centro de Aplicaciones Tecnológicas y Desarrollo Nuclear (CEADEN), Havana, Cuba¹⁰Centro de Investigaciones Energéticas Medioambientales y Tecnológicas (CIEMAT), Madrid, Spain¹¹Centro de Investigación y de Estudios Avanzados (CINVESTAV), Mexico City and Mérida, Mexico¹²Centro Fermi - Museo Storico della Fisica e Centro Studi e Ricerche "Enrico Fermi", Rome, Italy¹³Chicago State University, Chicago, Illinois, USA¹⁴China Institute of Atomic Energy, Beijing, China¹⁵COMSATS Institute of Information Technology (CIIT), Islamabad, Pakistan¹⁶Departamento de Física de Partículas and IGFAE, Universidad de Santiago de Compostela, Santiago de Compostela, Spain¹⁷Department of Physics, Aligarh Muslim University, Aligarh, India¹⁸Department of Physics, Ohio State University, Columbus, Ohio, USA¹⁹Department of Physics, Pusan National University, Pusan, Republic of Korea²⁰Department of Physics, Sejong University, Seoul, Republic of Korea²¹Department of Physics, University of Oslo, Oslo, Norway²²Department of Physics and Technology, University of Bergen, Bergen, Norway²³Dipartimento di Fisica dell'Università 'La Sapienza' and Sezione INFN, Rome, Italy²⁴Dipartimento di Fisica dell'Università and Sezione INFN, Cagliari, Italy²⁵Dipartimento di Fisica dell'Università and Sezione INFN, Trieste, Italy²⁶Dipartimento di Fisica dell'Università and Sezione INFN, Turin, Italy

- ²⁷*Dipartimento di Fisica e Astronomia dell'Università and Sezione INFN, Bologna, Italy*
- ²⁸*Dipartimento di Fisica e Astronomia dell'Università and Sezione INFN, Catania, Italy*
- ²⁹*Dipartimento di Fisica e Astronomia dell'Università and Sezione INFN, Padova, Italy*
- ³⁰*Dipartimento di Fisica 'E.R. Caianiello' dell'Università and Gruppo Collegato INFN, Salerno, Italy*
- ³¹*Dipartimento DISAT del Politecnico and Sezione INFN, Turin, Italy*
- ³²*Dipartimento di Scienze e Innovazione Tecnologica dell'Università del Piemonte Orientale and INFN Sezione di Torino, Alessandria, Italy*
- ³³*Dipartimento Interateneo di Fisica 'M. Merlin' and Sezione INFN, Bari, Italy*
- ³⁴*Division of Experimental High Energy Physics, University of Lund, Lund, Sweden*
- ³⁵*European Organization for Nuclear Research (CERN), Geneva, Switzerland*
- ³⁶*Excellence Cluster Universe, Technische Universität München, Munich, Germany*
- ³⁷*Faculty of Engineering, Bergen University College, Bergen, Norway*
- ³⁸*Faculty of Mathematics, Physics and Informatics, Comenius University, Bratislava, Slovakia*
- ³⁹*Faculty of Nuclear Sciences and Physical Engineering, Czech Technical University in Prague, Prague, Czech Republic*
- ⁴⁰*Faculty of Science, P.J. Šafárik University, Košice, Slovakia*
- ⁴¹*Faculty of Technology, Buskerud and Vestfold University College, Tonsberg, Norway*
- ⁴²*Frankfurt Institute for Advanced Studies, Johann Wolfgang Goethe-Universität Frankfurt, Frankfurt, Germany*
- ⁴³*Gangneung-Wonju National University, Gangneung, Republic of Korea*
- ⁴⁴*Gauhati University, Department of Physics, Guwahati, India*
- ⁴⁵*Helmholtz-Institut für Strahlen- und Kernphysik, Rheinische Friedrich-Wilhelms-Universität Bonn, Bonn, Germany*
- ⁴⁶*Helsinki Institute of Physics (HIP), Helsinki, Finland*
- ⁴⁷*Hiroshima University, Hiroshima, Japan*
- ⁴⁸*Indian Institute of Technology Bombay (IIT), Mumbai, India*
- ⁴⁹*Indian Institute of Technology Indore, Indore, India*
- ⁵⁰*Indonesian Institute of Sciences, Jakarta, Indonesia*
- ⁵¹*INFN, Laboratori Nazionali di Frascati, Frascati, Italy*
- ⁵²*INFN, Sezione di Bari, Bari, Italy*
- ⁵³*INFN, Sezione di Bologna, Bologna, Italy*
- ⁵⁴*INFN, Sezione di Cagliari, Cagliari, Italy*
- ⁵⁵*INFN, Sezione di Catania, Catania, Italy*
- ⁵⁶*INFN, Sezione di Padova, Padova, Italy*
- ⁵⁷*INFN, Sezione di Roma, Rome, Italy*
- ⁵⁸*INFN, Sezione di Torino, Turin, Italy*
- ⁵⁹*INFN, Sezione di Trieste, Trieste, Italy*
- ⁶⁰*Inha University, Incheon, Republic of Korea*
- ⁶¹*Institut de Physique Nucléaire d'Orsay (IPNO), Université Paris-Sud, CNRS-IN2P3, Orsay, France*
- ⁶²*Institute for Nuclear Research, Academy of Sciences, Moscow, Russia*
- ⁶³*Institute for Subatomic Physics of Utrecht University, Utrecht, Netherlands*
- ⁶⁴*Institute for Theoretical and Experimental Physics, Moscow, Russia*
- ⁶⁵*Institute of Experimental Physics, Slovak Academy of Sciences, Košice, Slovakia*
- ⁶⁶*Institute of Physics, Academy of Sciences of the Czech Republic, Prague, Czech Republic*
- ⁶⁷*Institute of Physics, Bhubaneswar, India*
- ⁶⁸*Institute of Space Science (ISS), Bucharest, Romania*
- ⁶⁹*Institut für Informatik, Johann Wolfgang Goethe-Universität Frankfurt, Frankfurt, Germany*
- ⁷⁰*Institut für Kernphysik, Johann Wolfgang Goethe-Universität Frankfurt, Frankfurt, Germany*
- ⁷¹*Institut für Kernphysik, Westfälische Wilhelms-Universität Münster, Münster, Germany*
- ⁷²*Instituto de Ciencias Nucleares, Universidad Nacional Autónoma de México, Mexico City, Mexico*
- ⁷³*Instituto de Física, Universidade Federal do Rio Grande do Sul (UFRGS), Porto Alegre, Brazil*
- ⁷⁴*Instituto de Física, Universidad Nacional Autónoma de México, Mexico City, Mexico*
- ⁷⁵*IRFU, CEA, Université Paris-Saclay, Saclay, France*
- ⁷⁶*iThemba LABS, National Research Foundation, Somerset West, South Africa*
- ⁷⁷*Joint Institute for Nuclear Research (JINR), Dubna, Russia*
- ⁷⁸*Konkuk University, Seoul, Republic of Korea*
- ⁷⁹*Korea Institute of Science and Technology Information, Daejeon, Republic of Korea*
- ⁸⁰*KTO Karatay University, Konya, Turkey*
- ⁸¹*Laboratoire de Physique Subatomique et de Cosmologie, Université Grenoble-Alpes, CNRS-IN2P3, Grenoble, France*
- ⁸²*Lawrence Berkeley National Laboratory, Berkeley, California, USA*

- ⁸³Moscow Engineering Physics Institute, Moscow, Russia
⁸⁴Nagasaki Institute of Applied Science, Nagasaki, Japan
⁸⁵National and Kapodistrian University of Athens, Physics Department, Athens, Greece
⁸⁶National Centre for Nuclear Studies, Warsaw, Poland
⁸⁷National Institute for Physics and Nuclear Engineering, Bucharest, Romania
⁸⁸National Institute of Science Education and Research, HBNI, Jatni, India
⁸⁹National Nuclear Research Center, Baku, Azerbaijan
⁹⁰National Research Centre Kurchatov Institute, Moscow, Russia
⁹¹Niels Bohr Institute, University of Copenhagen, Copenhagen, Denmark
⁹²Nikhef, Nationaal instituut voor subatomaire fysica, Amsterdam, Netherlands
⁹³Nuclear Physics Group, STFC Daresbury Laboratory, Daresbury, United Kingdom
⁹⁴Nuclear Physics Institute, Academy of Sciences of the Czech Republic, Řež u Prahy, Czech Republic
⁹⁵Oak Ridge National Laboratory, Oak Ridge, Tennessee, USA
⁹⁶Petersburg Nuclear Physics Institute, Gatchina, Russia
⁹⁷Physics Department, Creighton University, Omaha, Nebraska, USA
⁹⁸Physics department, Faculty of science, University of Zagreb, Zagreb, Croatia
⁹⁹Physics Department, Panjab University, Chandigarh, India
¹⁰⁰Physics Department, University of Cape Town, Cape Town, South Africa
¹⁰¹Physics Department, University of Jammu, Jammu, India
¹⁰²Physics Department, University of Rajasthan, Jaipur, India
¹⁰³Physikalisches Institut, Eberhard Karls Universität Tübingen, Tübingen, Germany
¹⁰⁴Physikalisches Institut, Ruprecht-Karls-Universität Heidelberg, Heidelberg, Germany
¹⁰⁵Physik Department, Technische Universität München, Munich, Germany
¹⁰⁶Research Division and ExtreMe Matter Institute EMMI, GSI Helmholtzzentrum für Schwerionenforschung GmbH, Darmstadt, Germany
¹⁰⁷Rudjer Bošković Institute, Zagreb, Croatia
¹⁰⁸Russian Federal Nuclear Center (VNIIEF), Sarov, Russia
¹⁰⁹Saha Institute of Nuclear Physics, Kolkata, India
¹¹⁰School of Physics and Astronomy, University of Birmingham, Birmingham, United Kingdom
¹¹¹Sección Física, Departamento de Ciencias, Pontificia Universidad Católica del Perú, Lima, Peru
¹¹²SSC IHEP of NRC Kurchatov institute, Protvino, Russia
¹¹³Stefan Meyer Institut für Subatomare Physik (SMI), Vienna, Austria
¹¹⁴SUBATECH, IMT Atlantique, Université de Nantes, CNRS-IN2P3, Nantes, France
¹¹⁵Suranaree University of Technology, Nakhon Ratchasima, Thailand
¹¹⁶Technical University of Košice, Košice, Slovakia
¹¹⁷Technical University of Split FESB, Split, Croatia
¹¹⁸The Henryk Niewodniczanski Institute of Nuclear Physics, Polish Academy of Sciences, Cracow, Poland
¹¹⁹The University of Texas at Austin, Physics Department, Austin, Texas, USA
¹²⁰Universidad Autónoma de Sinaloa, Culiacán, Mexico
¹²¹Universidade de São Paulo (USP), São Paulo, Brazil
¹²²Universidade Estadual de Campinas (UNICAMP), Campinas, Brazil
¹²³Universidade Federal do ABC, Santo Andre, Brazil
¹²⁴University of Houston, Houston, Texas, USA
¹²⁵University of Jyväskylä, Jyväskylä, Finland
¹²⁶University of Liverpool, Liverpool, United Kingdom
¹²⁷University of Tennessee, Knoxville, Tennessee, USA
¹²⁸University of the Witwatersrand, Johannesburg, South Africa
¹²⁹University of Tokyo, Tokyo, Japan
¹³⁰University of Tsukuba, Tsukuba, Japan
¹³¹Université Clermont Auvergne, CNRS/IN2P3, LPC, Clermont-Ferrand, France
¹³²Université de Lyon, Université Lyon 1, CNRS/IN2P3, IPN-Lyon, Villeurbanne, Lyon, France
¹³³Université de Strasbourg, CNRS, IPHC UMR 7178, F-67000 Strasbourg, France, Strasbourg, France
¹³⁴Università degli Studi di Pavia, Pavia, Italy
¹³⁵Università di Brescia, Brescia, Italy
¹³⁶V. Fock Institute for Physics, St. Petersburg State University, St. Petersburg, Russia
¹³⁷Variable Energy Cyclotron Centre, Kolkata, India
¹³⁸Warsaw University of Technology, Warsaw, Poland
¹³⁹Wayne State University, Detroit, Michigan, USA

¹⁴⁰*Wigner Research Centre for Physics, Hungarian Academy of Sciences, Budapest, Hungary*

¹⁴¹*Yale University, New Haven, Connecticut, USA*

¹⁴²*Yonsei University, Seoul, Republic of Korea*

¹⁴³*Zentrum für Technologietransfer und Telekommunikation (ZTT), Fachhochschule Worms, Worms, Germany*

[†]Deceased.

[‡]Also at Dipartimento DET del Politecnico di Torino, Turin, Italy.

[§]Also at M.V. Lomonosov Moscow State University, D.V. Skobeltsyn Institute of Nuclear, Physics, Moscow, Russia.

^{||}Also at Department of Applied Physics, Aligarh Muslim University, Aligarh, India.

[¶]Also at Institute of Theoretical Physics, University of Wrocław, Poland.